Clays and Clay Minerals, Vol. 34, No. 1, 17–24, 1986.

EFFECT OF HEATING ON MICROCRYSTALLINE SYNTHETIC GOETHITE

CHRISTIAN J. W. KOCH
Chemistry Department, Royal Veterinary and Agricultural University
DK-1871 Copenhagen V, Denmark

MORTEN BO MADSEN AND STEEN MØRUP
Laboratory of Applied Physics II, Technical University of Denmark
DK-2800 Lyngby, Denmark

GUNNAR CHRISTIANSEN AND LEIF GERWARD
Laboratory of Applied Physics III, Technical University of Denmark
DK-2800 Lyngby, Denmark

JØRGEN VILLADSEN
Haldor Topsøe Research Laboratories, DK-2800 Lyngby, Denmark

Abstract—The effect of heating synthetic microcrystalline goethite at 60°, 80°, and 105°C was studied by X-ray powder diffraction, electron microscopy, weight-loss measurements, and Mössbauer spectroscopy. Heating led to no detectable changes in the unit-cell parameters or crystallite size (210, 150, and 170 Å in the [020], [110], and [120] directions, respectively), however, some of the X-ray diffraction lines were broadened due to an increase in microstrain in these crystallographic directions. The superferromagnetic transition temperature increased from 43° to 46°, 53°, and 54°C after heating to 60°, 80°, and 105°C, respectively, showing that the desorption of water from the surfaces led to an enhanced magnetic coupling among the crystallites.

Key Words—Crystallite size, Goethite, Microstrain, Mössbauer spectroscopy, Thermal treatment, X-ray powder diffraction.

INTRODUCTION

The consensus of most studies of the thermal properties of natural and synthetic goethite (α-FeOOH) is that goethite is stable and unaffected by heating under various experimental conditions at temperatures below ~100°C. Heating to temperatures above ~100°C has generally been used for the determination of the amount of adsorbed water (Schulze and Schwertmann, 1984). Fey and Dixon (1981), however, reported that heating a sample of pure goethite at 110°C in air or in vacuo resulted in an increase of the crystallite size, as determined from the broadening of the X-ray powder diffraction profile, and proposed that the observed changes were caused by a decrease in the amount of adsorbed water.

Mørup *et al.* (1983) concluded from Mössbauer spectroscopy studies of two samples of synthetic microcrystalline goethite that the spectra of the samples could not be explained by a normal superparamagnetic behavior. Therefore, an attempt was made to explain the results on the basis of a model in which the magnetic coupling among the crystallites was taken into account. Such a system in which the magnetic coupling between neighboring microcrystals is significant and hinders superparamagnetic relaxation was described as "superferromagnetic" below the ordering temperature, T_p. The same term was used by Rancourt and Daniels (1984). Between T_p and the Curie or Néel temperature the system is superparamagnetic. Mørup *et al.* (1983) found that the Mössbauer results for the synthetic goethite samples could be explained by such a model of superferromagnetism. Inasmuch as the magnetic interaction among the crystallites depends on the distance between neighboring crystallites, it is likely that the crystallites will be more strongly magnetically coupled if water molecules are removed from the space between them by heating of the sample. Thus, Mössbauer spectroscopy appears to be a useful means of studying the effect of heating on microcrystalline goethite. The present work investigated the effect of heating on a sample of pure microcrystalline goethite between 40° and ~100°C.

MATERIALS AND METHODS

Materials

Synthetic goethite was grown from a partially neutralized iron nitrate solution having an initial pH of

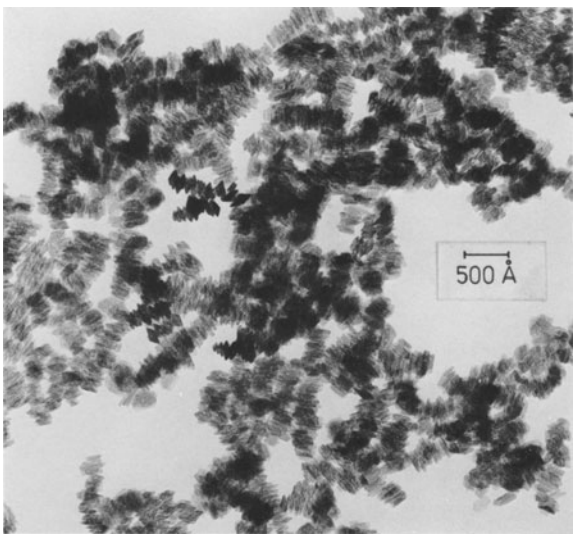

Figure 1. Electron micrograph of synthetic goethite sample 1B.

1.7, as described by Mørup *et al.* (1983). Weighed amounts of this material (sample 1), dried at 40°C, were heated in air in open containers at 60° (sample 1A) and 80°C (sample 1B) for six days and at 105°C (sample 1C) for four days. During the heating at 60°, 80°, and 105°C the samples lost 3.7, 5.0, and 3.8% weight, respectively. The temperatures and the duration of the heating were arbitrarily chosen to cover the temperature range between 40° and ~100°C; weight losses do not represent equilibrium losses.

A natural sample of well-crystallized goethite having crystallite sizes >10,000 Å, except along the [111] direction (~3000 Å) was studied as a reference. This sample contains impurities of <0.16% Si and <3000 ppm Al.

Transmission electron microscopy

Electron micrographs were obtained using a Jeol JEM 100B instrument operated at 80 kV. The samples were ultrasonically dispersed in water before the micrographs were obtained.

X-ray powder diffraction

X-ray powder diffraction (XRD) studies were performed on side-filled samples using a Philips PW 1050 goniometer equipped with variable slit, a graphite diffracted-beam monochromator, and CuK$\alpha_{1,2}$ radiation. A complete XRD pattern was obtained by line scanning. Important groups of diffraction lines were then chosen for profile analysis and recorded by step scanning using increments of 0.10°2θ and a fixed counting time of 40 s/step. The CuKα_2 contribution was removed from each measured profile using the Rachinger method (Klug and Alexander, 1974). The natural goethite sample was used to determine the broadening of the diffraction profile due to the finite experimental resolution.

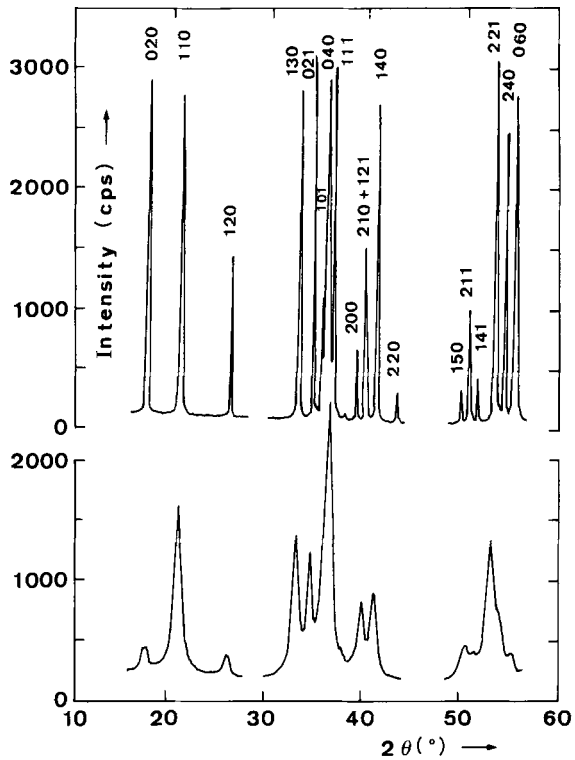

Figure 2. X-ray powder diffraction patterns of goethite. Upper diagram: natural sample. Lower diagram: sample 1. Weak diffraction at about 37.8°2θ is due to elemental Al from bottom of sample holder (CuK$\alpha_{1,2}$ radiation).

Mössbauer spectroscopy

Mössbauer spectra were obtained at temperatures between 10 and ~375 K (~150°C) using a constant acceleration Mössbauer spectrometer with a 50-mCi source of ^{57}Co in Rh. The spectrometer was calibrated by use of a 12.5-μm foil of α-Fe at room temperature. The Perspex (PMMA) absorber holders were sealed using epoxy resin, because it was found that sealing prevented irreversible changes in the samples during measurements at temperatures above the drying temperatures.

RESULTS

Electron micrographs

An electron micrograph of sample 1B is shown in Figure 1. The electron micrographs showed no significant changes upon heating of the sample. The samples exhibited extensive aggregation, and measurements of a few isolated particles gave dimensions of 100–200 Å. An electron micrograph of sample 1 was published earlier (Mørup *et al.*, 1983).

https://doi.org/10.1346/CCMN.1986.0340103 Published online by Cambridge University Press

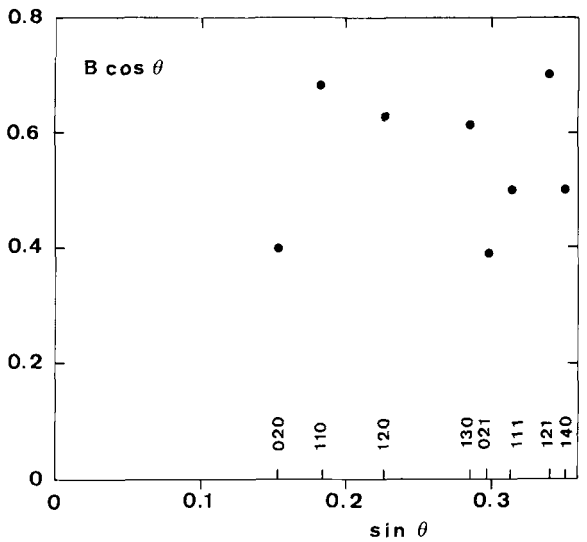

Figure 3. Williamson-Hall diagram of synthetic goethite (sample 1).

X-ray powder diffraction

Phase analysis. No phases other than goethite were detected in the XRD pattern of the samples (Figure 2). Unit-cell parameters are discussed below. The enhanced intensities of the 020, 040, and 060 reflections of the natural sample are likely due to preferred orientation.

Profile analysis for crystallite size and microstrain. Standard methods for analyzing combined size-strain broadening were difficult to apply to the present synthetic samples because of the absence of reflections of multiple orders and because of overlap of many lines, the latter leading to inaccuracies in the background determination (Klug and Alexander, 1974). In the present study of combined size-strain broadening the line profiles were analyzed by two approaches:

The first approach was to determine the full width at half maximum (FWHM), B (corrected for experimental broadening), for several reflections. In Figure 3 the results for sample 1 are displayed by means of a Williamson-Hall diagram, in which $B \cos\theta$ is plotted as a function of $\sin\theta$, θ being the Bragg angle. For an isotropic sample, the plot will give a straight line from which the crystallite size and the microstrain can be calculated (Williamson and Hall, 1953). The diagram shows a large scatter of points suggesting a marked anisotropy in crystallite size and microstrain. Thus, it was not possible to separate the size and strain contributions to line broadening using the Williamson-Hall method.

The second approach used the single-line method of analysis recently developed by Langford (1978), Keijser *et al.* (1982), and Delhez *et al.* (1982). The single-line analysis is based on the assumption that the size-broadened profile is described by a Cauchy function and the microstrain-broadened profile by a Gauss function. The observed diffraction profile is a convolution of these two functions, a so-called Voigt function. The breadth of the Cauchy and Gaussian components can be found from the ratio of the FWHM of the broadened profile to its integral breadth. This ratio is called the form factor of the Voigt function, and it ranges from 0.637 for a pure Cauchy function to 0.939 for a pure Gauss function. The crystallite size, D (Å), and the degree of microstrain, e (relative units), can then be calculated from the usual relations:

$$D = \lambda/(B_C \cos\theta) \quad (1)$$

$$e = B_G/(4 \tan\theta), \quad (2)$$

where B_C and B_G are the breadth on the 2θ scale (in radians) of the Cauchy and Gaussian components, respectively, θ is the Bragg angle, and λ is the X-ray

Table 1. Crystallite size (D) and microstrain (e) (relative units) of synthetic goethite estimated from a single-line Voigt analysis of the 020, 110, and 120 reflections.

	020		110		120	
Sample	D (Å)	e × 10³	D (Å)	e × 10³	D (Å)	e × 10³
1	210[1]	0[2]	150	6.0	170	7.1
1A	200	0	150	7.5	170	7.8
1B	220	0	150	10.	170	8.5
1C	200	0	140	11.	170	7.8

[1] Estimated standard deviation is 10 Å.
[2] Values given to the last significant figure.

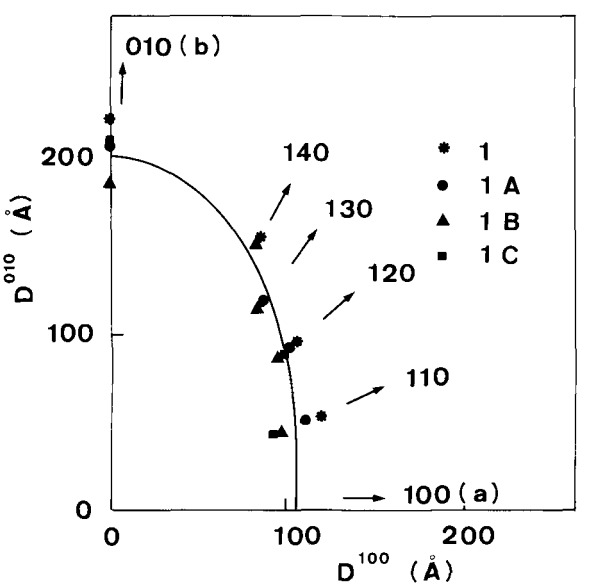

Figure 4. Polar diagram of the crystallite size of the synthetic goethites in the (001) plane. Arrows indicate the directions normal to the lattice planes with given Miller indices. D^{010} = dimension in [010] direction. D^{100} = dimension in [100] direction.

https://doi.org/10.1346/CCMN.1986.0340103 Published online by Cambridge University Press

Table 2. Unit-cell dimensions of goethite.

Sample	*a* (Å)	*b* (Å)	*c* (Å)	V (Å³)
Natural	4.602 (1)[1]	9.958 (1)	3.022 (1)	138.49 (3)
Synthetic				
1	4.608 (9)	9.956 (9)	3.027 (4)	138.9 (3)
1A	4.603 (9)	9.953 (9)	3.026 (4)	138.7 (3)
1B	4.601 (9)	9.953 (9)	3.026 (4)	138.6 (3)
1C	4.606 (9)	9.957 (9)	3.026 (4)	138.8 (3)

[1] The uncertainties, given in parenthesis, are the standard deviations of the least squares fit.

wavelength. The Scherrer constant was set to unity in the present work.

Table 1 shows the crystallite size and the degree of microstrain obtained from the single-line Voigt analysis of the 020, 110, and 120 reflections, the only ones suitable in the present study. An anisotropy in both size and degree of microstrain can be seen, in accord with the Williamson-Hall plot (Figure 3). For a given crystallographic direction the crystallite size was practically independent of the heat treatment. The degree of microstrain along the *b* axis (020 reflection) was below the detection limit and independent of the heat treatment, whereas for the two other directions the degree of microstrain generally increased with the heating temperature. For the direction normal to the (120) planes, however, a decrease in microstrain was found following heating at the highest temperature.

The range of the form factors for the 020, 110, and 120 reflections was between 0.64 and 0.77 showing that the broadening of these lines was mainly due to change of crystallite size. Assuming that line broadening due to crystallite size was predominant for all reflections, the diffraction profiles were fitted to pure Cauchy functions. Figure 4 is a polar diagram of crystallite size estimated in this way along different directions in the (001) plane. The size is about 100 Å along the *a* axis and 200 Å along the *b* axis. No size determination along the *c* axis was possible. Four different diffraction vectors making angles of about 30° with the *c* axis gave crystallite sizes in the range 100–200 Å.

Unit-cell parameters. The orthorhombic unit-cell parameters (space group *Pbnm*) of the samples were calculated by a least squares fit to the 2θ positions of the diffraction lines (Table 2). The positions of the XRD lines were first corrected for small shifts caused by the slightly asymmetric diffraction profile (Reynolds, 1968; Trunz, 1976; Schulze, 1984). The 120 line shifted $0.03°2\theta$, but all other lines shifted by no more than $0.01°2\theta$. For the natural sample, all line positions were used in the calculation of unit-cell parameters; however, for the synthetic samples fewer line positions were used because of uncertainties in the fitting of their positions, due to overlapping diffraction lines. These uncertainties in part explain the greater standard deviations of the unit-cell parameters found for the synthetic samples.

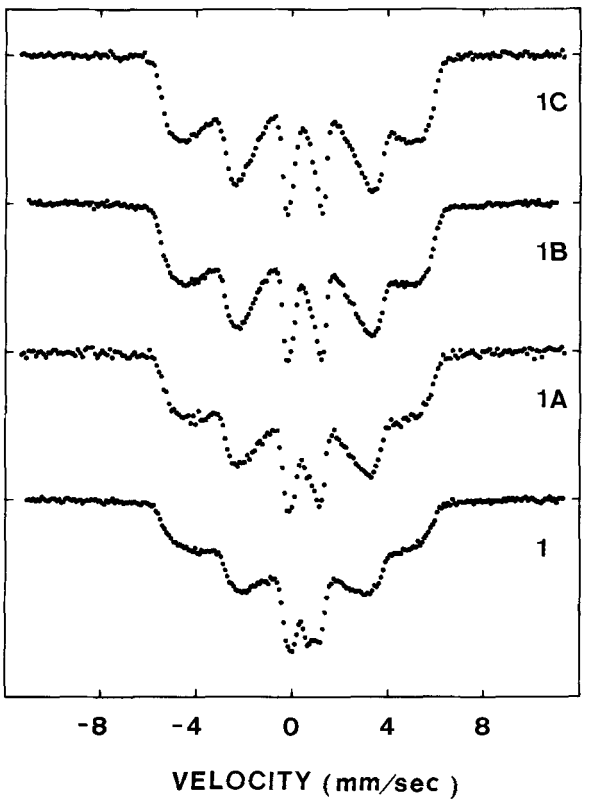

Figure 5. Mössbauer spectra of the samples of synthetic goethite at 298 K.

Mössbauer spectroscopy

Differences in the Mössbauer spectra of the heated synthetic samples were most clearly revealed by comparing the spectra taken at temperatures slightly below the transition temperature, T_p, at which the six-line pattern collapsed into a doublet. For sample 1, T_p = 316 K (Mørup *et al.*, 1983). Figure 5 shows the spectra obtained at 298 K (25°C). All spectra showed a line broadening typical of microcrystalline goethite (Murad and Schwertmann, 1983; Mørup *et al.*, 1983 and references therein). With increasing heating temperature of the synthetic samples the magnetic hyperfine splitting in the spectra became better resolved, and the average hyperfine field increased. In the temperature range 310–330 K the magnetic splitting of the spectra collapsed into a quadrupole doublet. Spectra of the four synthetic samples obtained at 319 K (46°C) (Figure 6) show that at this temperature the magnetic splitting collapsed for samples 1 and 1A. The spectra of samples 1B and 1C show a quadrupole doublet superimposed on a broad magnetic component. The asymmetry of the doublets in Figure 6 is presumably due to relaxation

https://doi.org/10.1346/CCMN.1986.0340103 Published online by Cambridge University Press

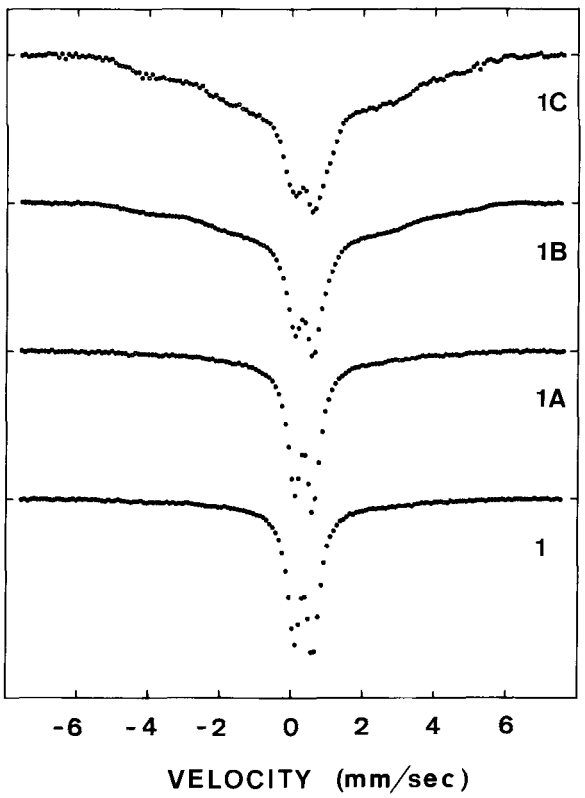

Figure 6. Mössbauer spectra of the samples of synthetic goethite at 319 K.

effects and will be discussed elsewhere. The Néel temperature of well-crystallized goethite is about 393.5 K (Woude and Dekker, 1966; Mørup *et al.*, 1983). Therefore, the collapse of the magnetic splitting in the present spectra at less than 330 K must have been due to fast superparamagnetic relaxation.

The distributions in magnetic hyperfine fields of the magnetically split spectra were calculated using the computer program developed by Wivel and Mørup (1981); the average hyperfine fields of these distributions were also calculated. The distributions obtained from the spectra of samples 1 and 1B at 298 K are shown in Figure 7, in which the peaks at about 3.0 T indicate the presence of paramagnetic components in the spectra.

As in previous studies (Mørup *et al.*, 1983 and references therein) of microcrystalline goethite, the average hyperfine fields were found to be substantially smaller than the bulk value, except at very low temperatures where they approached the bulk value.

DISCUSSION

Unit-cell parameters

The unit-cell parameters of the natural sample (Table 2) are close to those published by Sampson (1969) and Harrison *et al.* (1975), showing that this sample is well crystallized and thus well suited as a reference in the studies of the properties of the synthetic samples. Within the limits of uncertainty the unit-cell parameters for the four synthetic samples were identical and very close to those of the natural sample showing that: (1) the synthetic samples consisted of crystalline goethite particles, and (2) heating of synthetic microcrystalline goethite at temperatures up to 105°C did not change the unit-cell parameters. The latter finding is in accordance with the results of Fey and Dixon (1981), who found no change in the unit-cell parameters of a synthetic goethite after heating a sample to 110°C. Schulze (1984) reported unit-cell parameters for synthetic, unsubstituted goethites similar to those found in the present study.

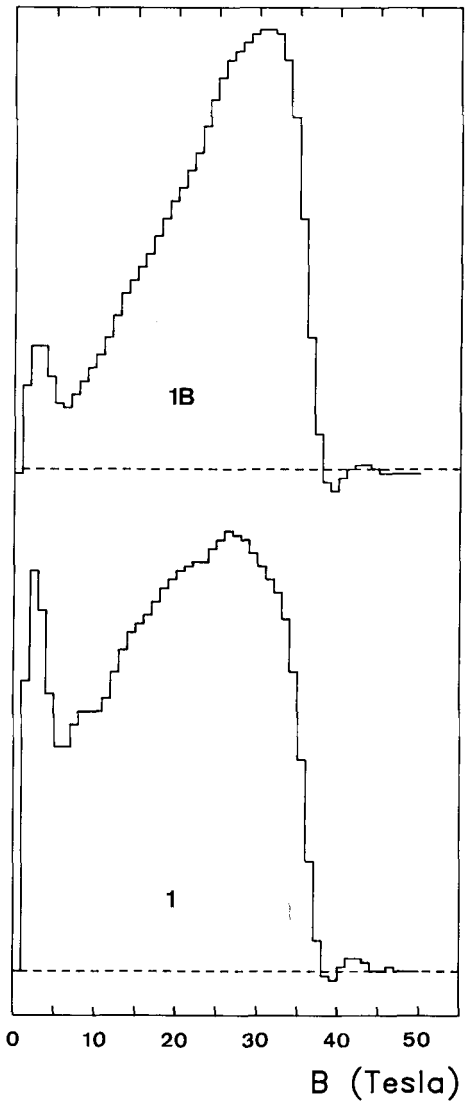

Figure 7. Magnetic hyperfine field distributions of synthetic goethites (samples 1 and 1B) at 298 K.

https://doi.org/10.1346/CCMN.1986.0340103 Published online by Cambridge University Press

Crystallite size and microstrain

As shown by the data in Table 1 the crystallites did not change size on heating. The data points in Figure 4 along the directions normal to the (110) and (120) planes may indicate shrinking of the crystallites following heating, but this apparent shrinking was most likely due to our neglect of the increased strain contribution to line broadening in the data analysis. Contrary to the present results, Fey and Dixon (1981) found that heating their sample to 110°C resulted in a narrowing of the XRD lines, which they interpreted as being due to an increase of the crystallite size. Their results, however, may also be explained by an annihilation of microstrain in the crystallites at temperatures above ~100°C.

Table 1 shows a negligible amount of microstrain along the *b* axis, whereas along directions normal to the (110) and (120) planes a considerable amount of microstrain was noted. Furthermore, the different magnitude of changes in the value of microstrain given by the 110 and 120 reflections also suggests that the microstrain mainly was along the *a* axis. This finding is in accord with the defect crystal model proposed by Schulze (1984), who suggested that bonding along the *a* axis is less rigid compared to the *b* and *c* axes because of preferential hydrogen bonding in the *a* direction. Consequently, the crystallites may accommodate microstrain more easily along the *a* axis. Microstrain of similar order of magnitude as found in the present study was reported by Gónez-Villacieros *et al.* (1984) in samples of maghemite (γ-Fe_2O_3).

As suggested by the XRD profile analysis, the crystallites had dimensions of ~200 Å in the longest and ~100 Å in the shortest directions. These dimensions are comparable with the dimensions observed in TEM indicating that each particle is a single crystallite.

Magnetic properties

Superferromagnetism. The Mössbauer results were analyzed on the basis of the model for superferromagnetism developed earlier (Mørup, 1983; Mørup *et al.*, 1983). Thus, the magnetic anisotropy energy was assumed to be negligible compared to the magnetic interaction energy, and the interaction energy between two crystallites i and j, E_{ij}, was assumed to be of the form:

$$E_{ij} = -K_m \vec{M}_i(T) \cdot \vec{M}_j(T), \qquad (3)$$

where K_m is the coupling constant for the magnetic coupling between the crystallites, which may have contributions from both magnetic dipolar interaction and exchange interaction between pairs of atoms at the interface between two neighboring crystallites, and $\vec{M}_i(T)$ and $\vec{M}_j(T)$ are the sublattice magnetization vectors of the crystallites i and j, respectively, at the absolute temperature, T. According to this model, the normalized hyperfine field (i.e., the average hyperfine field divided by the bulk hyperfine field obtained at the same temperature) follows the function b(T), which is derived from the expression (Mørup *et al.*, 1983):

$$b(T) = L\left\{\frac{3T_p}{T}\left[\frac{B_0(T)}{B_0(T_p)}\right]^2 b(T)\right\}. \qquad (4)$$

Here L{ } is the Langevin function, T_p is the temperature at which the magnetic splitting collapses, and $B_0(T)$ is the bulk magnetic hyperfine field of goethite. The temperature T_p is given by (Mørup, 1983; Mørup *et al.*, 1983):

$$T_p = K_m M_0^2(T_p)/3k, \qquad (5)$$

where $M_0(T)$ is the sublattice magnetization of bulk samples and k is Boltzmann's constant.

The Mössbauer results for all four synthetic samples can be explained on the basis of the superferromagnetism model. The value of T_p, obtained from the fits, are 43° (316), 46° (319), 53° (326), and 54°C (327 K) for samples 1, 1A, 1B, and 1C, respectively. Figure 8 shows the normalized hyperfine fields, b(T) as a function of temperature for samples 1 and 1B, and the best fits with the model for superferromagnetism. In the theoretical model, the influence of magnetic anisotropy and crystallite size on the magnetic properties of the samples were neglected, and the magnetic coupling among the crystallites was assumed to be the only important parameter. Changes in crystallite size and magnetic anisotropy, however, could also have changed the value of T_p derived from the fits of the type shown in Figure 8. Although a change in crystallite volume upon heating might have been expected, the XRD profile analysis indicated no change in the crystallite size.

Mørup *et al.* (1982) showed that the surface contribution to the magnetic anisotropy energy constant in microcrystals of Fe, Co, Ni, and Fe_3O_4 may change when molecules are adsorbed or desorbed. Therefore, the release of water from the surface of goethite crystallites during heating might have changed the magnetic anisotropy energy constant. The microstrain induced by the heating might also have changed the magnetic anisotropy energy constant. The fits of the average hyperfine field with the model for superferromagnetism (Figure 8) indicate, however, that the magnetic interaction energy was much larger than the magnetic anisotropy energy. Therefore, the increase in T_p with increasing heating temperature was most likely due to an enhanced magnetic interaction among the crystallites. The weight loss on heating, due to the loss of adsorbed water, also suggests that the crystallites were in closer proximity after heating. The weight loss corresponds to an average desorption of one or two layers of water from the surface of the crystallites.

Magnetic dipolar interaction. The magnetic dipolar interaction between two perfect antiferromagnetic crystals is negligible; however, a microcrystal of an anti-

https://doi.org/10.1346/CCMN.1986.0340103 Published online by Cambridge University Press

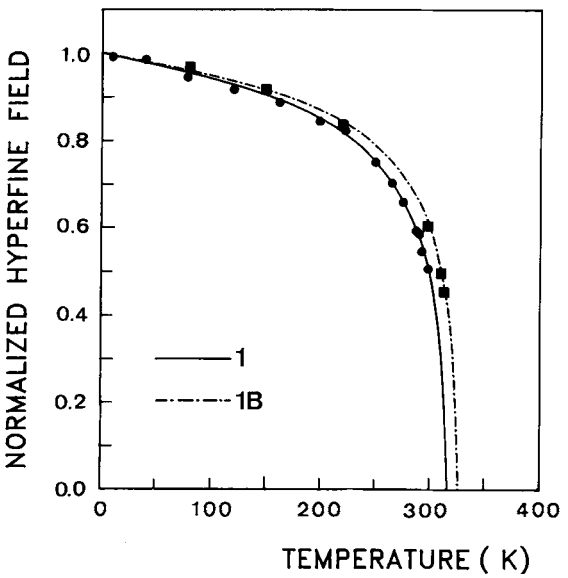

Figure 8. Temperature dependence of the normalized hyperfine fields of synthetic goethites (sample 1 and 1B).

ferromagnetic material with N magnetic atoms is expected to possess a magnetic moment proportional to a factor of the order of $\langle S_z \rangle N^{1/2}$, where S is the spin of the atoms (Néel, 1961). The magnetic moment, μ, can be expressed as:

$$\mu \approx 2M_0(T)VN^{1/2}/z, \tag{6}$$

where z is the number of iron atoms in the unit cell (=4 in goethite) and V is the volume of the unit cell. The magnetic dipole interaction energy is of the order of:

$$E_d \approx -\frac{\mu_0\mu^2}{4\pi r^3} = -\frac{\mu_0 4V^2}{4\pi z^2 r^3} NM_0^2(T), \tag{7}$$

where μ_0 is the vacuum permeability and r is the distance between two crystallites, which, according to the electron micrographs is of the order of 100 Å (center to center). Thus, assuming that the magnetic coupling is solely due to magnetic dipolar interactions, from Eqs. (3) and (7):

$$K_m = \frac{\mu_0 4V^2}{4\pi z r^3} N. \tag{8}$$

Using the numerical values for the present goethite samples in Eq. (5), $T_p \approx 0.2$ K, i.e., T_p is smaller than the experimental value by more than two orders of magnitude. Therefore, the magnetic dipole interaction seems not to be able to explain the Mössbauer results; however, inasmuch as the uncompensated magnetic dipoles in antiferromagnetic microcrystals should be located mainly at the surface (Néel, 1961), the effective value of r may be smaller than assumed above, thereby leading to a larger value of K_m. Thus, the magnetic dipolar interaction may not be negligible.

Exchange coupling. The exchange coupling between two crystallites cannot be calculated directly because it depends critically on the overlap of the electronic wave functions of surface atoms belonging to the two crystallites. Instead, for the present data, the average exchange-coupling constant was calculated from the experimental value of T_p, assuming that the exchange coupling was predominant. Thus, Eq. (3) was rewritten as:

$$E = -\sum_{ij} 2J^{ij}\vec{S}_i \cdot \vec{S}_j, \tag{9}$$

where J^{ij} is the exchange coupling constant for the interaction between two atoms, and the summation is taken over all interacting pairs of atoms belonging to the two neighboring crystallites. Because only a rough estimate of the average value of the magnetic coupling constant was required, Eq. (9) was rewritten as:

$$E \approx -2J \cdot N_s \langle S_z \rangle^2, \tag{10}$$

where N_s is the number of interacting pairs of atoms and J was the average coupling constant. N_s was assumed to be equal to the number of iron atoms in the surface layer. Using this model:

$$T_p = \frac{2JN_s\langle S_z \rangle^2}{3k}. \tag{11}$$

On the basis of the electron micrographs and the XRD results N_s was estimated to be ~1500. Because $T_p \approx$ 47°C (320 K), from Eq. (11), $J/k \approx 0.1$ K.

This average exchange coupling constant is of the same order of magnitude as those found in compounds with Curie or Néel temperatures of the order of 1–10 K. Magnetic transition temperatures of this magnitude are not unusual in, for example, hydrated iron salts, in which the iron atoms are separated by water molecules. Thus, the present results for goethite may be explained by an exchange coupling among surface atoms in neighboring crystallites through a thin layer of water molecules. Because the surfaces were presumably not perfectly smooth, the values of J^{ij} presumably varied substantially for the individual pairs of atoms, and the main contribution to the magnetic interaction among the crystallites probably arose from a small number of "exchange bridges" between the crystallites.

CONCLUSIONS

On the basis of XRD and TEM analyses the synthetic goethite samples used in this study were found to consist of crystalline goethite particles having crystallite dimensions of about 100–200 Å. No change in the crystallite size was detected after heating, showing that the crystallites did not sinter on heating. Using three reflections to estimate the combined strain-crystallite size broadening effect on the XRD lines, the microstrain in the crystallites was found to be different along different crystallographic directions and the value of the microstrain changed along some directions after

https://doi.org/10.1346/CCMN.1986.0340103 Published online by Cambridge University Press

the heat treatment. The Mössbauer results support a superferromagnetism model for the magnetically interacting crystallites and indicate an increased magnetic coupling among the microcrystals after heating, presumably because of desorption of water from the space between neighboring crystallites. The predominant contribution to the magnetic coupling was probably due to exchange interaction between surface atoms belonging to neighboring crystallites. The present study shows the necessity of specifying the drying procedure used in studies of iron oxide materials, as this procedure significantly influences the physical properties of the final product.

ACKNOWLEDGMENT

We thank B. Bloch for preparing the electron micrographs.

REFERENCES

Delhez, R., Keijser, Th. H. de, and Mittemeijer, E. J. (1982) Determination of crystallite size and lattice distortions through X-ray diffraction line profile analysis: *Fresenius Z. Anal. Chem.* **312,** 1–16.

Fey, M. V. and Dixon, J. B. (1981) Synthesis and properties of poorly crystalline hydrated aluminous goethites: *Clays & Clay Minerals* **29,** 91–100.

Gómez-Villacieros, R., Hernán, L., Morales, J., and Tirado, J. L. (1984) Textural evolution of synthetic γ-FeOOH during thermal treatment by differential scanning calorimetry: *J. Colloid Interface Sci.* **101,** 392–400.

Harrison, R. K., Aitkenhead, N., Young, B. R., and Dagger, P. F. (1975) Goethite from Hindlow, Derbyshire: *Bull. Geol. Surv. Great Britain* **52,** 51–54.

Keijser, Th. H. de, Langford, J. I., Mittemeijer, E. J., and Vogels, A. B. P. (1982) Use of the Voigt function in a single-line method for the analysis of X-ray diffraction line broadening: *J. Appl. Cryst.* **15,** 308–314.

Klug, H. P. and Alexander, L. E. (1974) *X-ray Diffraction Procedures for Polycrystalline and Amorphous Materials:* Wiley, New York, 966 pp.

Langford, J. I. (1978) A rapid method for analysing the breadths of diffraction and spectral lines using the Voigt function: *J. Appl. Crystallogr.* **11,** 10–14.

Murad, E. and Schwertmann, U. (1983) The influence of aluminium substitution and crystallinity on the Mössbauer spectra of goethite: *Clay Miner.* **18,** 301–312.

Mørup, S. (1983) Magnetic hyperfine splitting in Mössbauer spectra of microcrystals: *J. Magn. Magn. Mat.* **37,** 39–50.

Mørup, S., Madsen, M. B., Franck, J., Villadsen, J., and Koch, C. J. W. (1983) A new interpretation of Mössbauer spectra of microcrystalline goethite: "super-ferromagnetism" or "super-spin-glass" behaviour?: *J. Magn. Magn. Mat.* **40,** 163–174.

Mørup, S., Topsøe, H., and Clausen, B. S. (1982) Magnetic properties of microcrystals studied by Mössbauer spectroscopy: *Phys. Scr.* **25,** 713–719.

Néel, L. (1961) Superparamagnétisme des grains très fins antiferromagnétiques: *Comp. Rend. Acad. Sci. Paris* **252,** 4075–4080.

Rancourt, D. G. and Daniels, J. M. (1984) Influence of unequal magnetization direction probabilities on the Mössbauer spectra of superparamagnetic particles: *Phys. Rev. B* **29,** 2410–2414.

Reynolds, R. C. (1968) The effect of particle size on apparent lattice spacings: *Acta Crystallogr.* **A24,** 319–320.

Sampson, C. F. (1969) The lattice parameters of natural single crystal and synthetically produced goethite (α-FeOOH): *Acta Crystallogr.* **B25,** 1683–1685.

Schulze, D. G. (1984) The influence of aluminum on iron oxides. VIII. Unit-cell dimensions of Al-substituted goethites and estimation of Al from them: *Clays & Clay Minerals* **32,** 36–44.

Schulze, D. G. and Schwertmann, U. (1984) The influence of aluminium on iron oxides: X. Properties of Al-substituted goethites: *Clay Miner.* **19,** 521–539.

Trunz, V. (1976) The influence of crystallite size on the apparent basal spacings of kaolinite: *Clays & Clay Minerals* **24,** 84–87.

Williamson, G. K. and Hall, W. H. (1953) X-ray line broadening from filed aluminium and wolfram: *Acta Met.* **1,** 22–31.

Wivel, C. and Mørup, S. (1981) Improved computational procedure for evaluation of overlapping hyperfine parameter distributions in Mössbauer spectra: *J. Phys. E: Sci. Instrum.* **14,** 605–610.

Woude, F. van der and Dekker, A. J. (1966) Mössbauer effect in α-FeOOH: *Phys. Stat. Sol.* **13,** 181–193.

(Received 18 January 1985; accepted 12 October 1985; Ms. 1444)